Desalination and Water Treatment
www.deswater.com
doi: 10.1080/19443994.2015.1008580

57 (2016) 5740–5752
March

Taylor & Francis
Taylor & Francis Group

Synthesis of itaconic acid—sodium allysulfonate—sodium hypophosphite copolymer and evaluation of its scale and corrosion inhibition performance

Zhenfa Liu[a,c,*], Haolin Fu[a,b,c], Lihui Zhang[a,c], Haihua Li[a,c], Xuan Liu[a,b,c]

[a]*Institute of Energy Sources, Hebei Academy of Science, Shijiazhuang 050081, Hebei, China, Tel. +86 13703390640; Fax: +86 0311 83031008; email: lzf63@sohu.com (Z. Liu), Tel. +86 15833990331; email: haolin5151585@126.com (H. Fu), Tel. +86 13513388856; email: zlhkxy@sohu.com (L. Zhang), Tel. +86 13784383035; email: c.t.0205@sina.com (H. Li), Tel. +86 15831191166; email: xuanlx_0907@163.com (X. Liu)*
[b]*School of Chemical Engineering, Hebei University of Technology, Tianjin 300130, China*
[c]*Hebei Engineering Research Center for Water Saving in Industry, Shijiazhuang 050081, Hebei, China*

Received 2 July 2014; Accepted 27 December 2014

ABSTRACT

A novel biodegradable multifunctional scale and corrosion inhibitor containing carboxylic acid, sulpfonic acid, and phosphonic acid groups was synthesized from the monomers of itaconic acid (IA), sodium allysulfonate (SAS), and sodium hypophosphite (SHP) by oxidation–reduction initiator system. The optimum synthesis conditions were determined by orthogonal experiments. The performances of scale and corrosion inhibition, dispersion, and biodegradability of the IA/SAS/SHP copolymer were studied. The results showed that the IA/SAS/SHP copolymer has good performances of scale and corrosion inhibition, dispersion performance on ferric oxide, and biodegradability. When the concentration of IA/SAS/SHP copolymer was 20 mg/L, the scale inhibition rate was 95.1%. When the concentration of the IA/SAS/SHP copolymer was 60 mg/L, the corrosion rate was 0.02823 mm/a and the corrosion inhibition rate reaches above 90%. The $CaCO_3$-scale samples and the corrosion testing pieces were observed and analyzed by SEM. The IA/SAS/SHP copolymer could destroy the growth habits of the crystal and lead to crystal distortion.

Keywords: IA/SAS/SHP copolymer; Synthesis; Scale inhibition; Corrosion inhibition

1. Introduction

Circulating cooling water system is widely used in industrial processes. The construction materials of this system are mainly carbon steel and stainless steel [1,2]. Some problems, for instance, scale and corrosion in cooling water systems may appear, when natural water is used as thermal fluid [3]. The scale not only degrades performance of heat exchangers, but also wastes energy [4–6]. Corrosion will cause the deterioration of equipment and result in great economic loss and catastrophic accidents [7,8]. In order to control these problems, scale and corrosion inhibitors have been successfully developed [9,10]. However, the scale and corrosion inhibitor used currently possess unsatisfactory overall performance and cause secondary pollution, which restricts their application in industry [11]. As a result, intense attention is being paid to environmentally friendly scale and corrosion inhibitor [12–14].

*Corresponding author.

Itaconic acid (IA) homopolymer is recognized as a green water treatment agent for its biodegradability [15]. IA homopolymer contains carboxylic group with good chelating ability, making it feasible to absorb or combine with metal ions such as Ca^{2+}, thereby preventing $CaCO_3$ deposition [16]. But the IA homopolymer has not been used widely in the cooling water systems. This is because its performances of corrosion inhibition and dispersion are not good [17]. To improve its performance, the IA/sodium allysulfonate (SAS)/sodium hypophosphite (SHP) was synthesized.

In the present research, we intend to introduce sulfonic acid and phosphonic acid groups to the molecular structure of IA homopolymer by means of graft copolymerization to improve the corrosion inhibition and dispersion performance of resultant grafted copolymer. The copolymer can be used separately without combination with other agent to overcome the corrosion and scale problems as well as precipitation of ferric oxide in open recirculating cooling systems, compared with traditional water treatment agents. There are not relevant references about the IA/SAS/SHP copolymer as corrosion and scale inhibitor in the literature. The IA/SAS/SHP copolymer is a novel efficient environmentally friendly multifunctional scale and corrosion inhibitor. It is convenient and economical and it has a practical value and possibly a bright prospect. In this work, the IA/SAS/SHP copolymer was synthesized from the monomers of IA, SAS, and SHP by oxidation–reduction initiator system. The structure of the copolymer was characterized by means of Fourier transform infrared (FTIR) spectrometry and nuclear magnetic resonance (NMR) spectroscopy. The performances of scale and corrosion inhibition, dispersion, and biodegradability of the IA/SAS/SHP copolymer were investigated. Its effect on the formation of $CaCO_3$ crystal was studied by means of scanning electron microscopy (SEM) and X-ray diffraction (XRD).

2. Experimental

2.1. Materials and instruments

IA was purchased from Huaming Biochemistry Co., Ltd (Jinan, China). SAS was obtained from Zibo Zhangdian Xiangrang Chemical Plant (Shandong, China). SHP was obtained from Hongyan Chemical Reagent Factory (Tianjin, China). Ammonium ferrous sulfate was supplied by Beijing Chemical Reagent Third Factory (Beijing, China). Isopropanol was supplied by Bodi Chemical Reagent Co. Ltd (Tianjin, China). H_2O_2 was purchased from Baishi Chemical Reagent Co. Ltd (Tianjin, China). $CaCl_2{\cdot}2H_2O$ and $NaHCO_3$ were purchased from Kemiou Chemical Reagent Co. Ltd (Tianjin, China). IA and SAS were of technical grade, and all other chemicals were of analytical reagent grade.

Instruments used in the present research included a Shanghai Optical Instrument 724 spectrophotometer, Perkin-Elmer SP100 FTIR spectrometer, Xinyou Instrument Factory RCC-I rotation coupon corrosion tester, Elementar vario MICRO cube elementary analyzer, Rigaku Ultima IV X-ray diffractometer, and FEI Inspect S50 SEM.

2.2. Preparation of IA/SAS/SHP copolymer

2.2.1. Synthesis of IA/SAS/SHP copolymer

About 52 g (or 48.75 g, 54.2 g) of IA, 13 g (or 16.25 g, 10.8 g) of SAS, 2 mL isopropanol, and 2 g of ammonium ferrous sulfate were added into deionized water and was stirred till they become completely transparent. The solution was heated to 90℃ (or 95℃, 100℃), then 7.15 g (or 3.25 g, 5.2 g) of NaH_2PO_2 and 30 mL hydrogen peroxide were added to the above solution slowly in 1.5 h. Then the solution was heated to 102℃ and maintained for 2 h, the IA/SAS/SHP copolymer was obtained. Synthesis route of the IA/SAS/SHP copolymer is shown in Fig. 1.

2.2.2. Purification and characterization of IA/SAS/SHP copolymer

The IA/SAS/SHP copolymer solution and alcohol were mixed and stirred. The precipitation of IA/SAS/SHP copolymer was recovered by filtration and dried at 60℃ in a drying cabinet for 4 h.

The molecular skeleton structure was determined by FTIR, the scan area was 400–4,000 cm^{-1}. The formular weight of the IA/SAS/SHP copolymer was measured by the viscosity method. The product was diluted to 0.1% (wt.%) with sodium thiocyanate. The viscosity of this solution was determined by an Ubbelohde viscometer supplied by Liangjing Glass Instrument Factory (Shanghai, China). The measure temperature was (30 ± 0.3)℃. The intrinsic viscosity number was calculated by Eq. (1).

$$[\eta] = \frac{\sqrt{2(\eta_{sp} - \ln \eta_r)}}{\rho} = \frac{\sqrt{2[(\frac{t}{t_0} - 1) - \ln \frac{t}{t_0}]}}{\rho} \quad (1)$$

where η_{sp} is specific viscosity, $\eta_{sp} = (t - t_0)/t_0$; η_r is relative viscosity, $\eta_r = t/t_0$; ρ is mass concentration of measure solution, g/dL; t_0 is the time of sodium

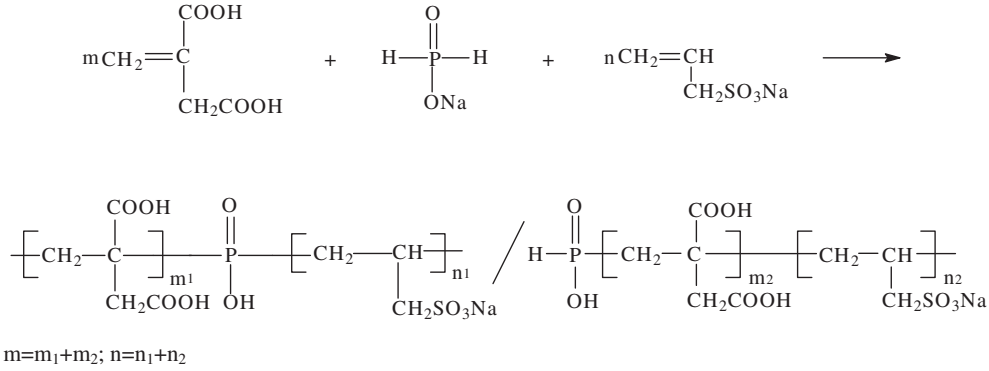

Fig. 1. Synthesis route to IA/SAS/SHP copolymer.

thiocyanate solution flowing through the viscometer, *s*; *t* is the time of the measure solution flowing through the viscometer, *s*.

According to Mark–Houwink empirical formula, the relative molecular mass of products can be calculated by intrinsic viscosity number.

$$[\eta] = KM^{\alpha} \tag{2}$$

where $K = 1.51 \times 10^{-3}$, $\alpha = 0.82$.

2.2.3. Orthogonal experiment

In this work, effects of selected factors were studied through the use of L_9 (3^4) orthogonal experiment and optimal conditions for preparing the IA/SAS/SHP copolymer were obtained. In L_9 (3^4) matrix, which was an orthogonal array of four factors and three levels, nine trials were carried out according to the matrix to complete the optimization process. Each row of orthogonal array represents a run, which is a specific set of factor levels to be tested. The run order of the trials is randomized to avoid any personal or subjective bias.

There are two important parameters in a range analysis of the orthogonal experiment: K_{ji} and R_j. K_{ji} is defined as the sum of the evaluation indexes of all levels (i, $i = 1, 2, 3$) in each factor (j, $j = A, B, C, D$) and k_{ji} (mean value of K_{ji}) is used to determine the optimal level and the optimal combination of factors. The optimal level for each factor could be obtained when k_{ji} is the largest. R_j is defined as the range between the maximum and minimum values of k_{ji}, and is used for evaluating the importance of the factors, i.e. a larger R_j means a greater importance of the factor [18].

2.3. Inhibition performance of IA/SAS/SHP copolymer against $CaCO_3$ scale

Static-scale inhibition experiments were conducted according to China National Standard method (GB/T 16632-2008) to evaluate the scale inhibition efficiency of synthesized IA/SAS/SHP copolymer against $CaCO_3$ scale [19]. Briefly, in a conical flask (capacity of 0.5 L) was prepared an aqueous solution containing 600 mg/L Ca^{2+} and 1,200 mg/L HCO_3^-. The obtained solution was uniformly mixed with a known amount of the IA/SAS/SHP copolymer and allowed to react in a water bath at 80°C for 10 h. At the end of the reaction, the obtained mixed solution was collected and cooled to room temperature. The concentration of Ca^{2+} in the solution was measured using EDTA titration. The scale inhibition efficiency of the IA/SAS/SHP copolymer against $CaCO_3$ scale was calculated as Eq. (3) [20]:

$$\eta = \frac{V_1 - V_0}{V_2 - V_0} \times 100\% \tag{3}$$

where V_0 (mL) is the volume of EDTA consumed by a certain amount of calcium cation in the absence of scale inhibitor in to-be-tested solution (control test); V_1 is the volume of EDTA consumed by a certain amount of calcium cation in the presence of scale inhibitor in to-be-tested solution; and V_2 is the volume of EDTA consumed by all calcium cations in to-be-tested solution [21].

2.4. Ability of IA/SAS/SHP to disperse ferric oxide

A solution containing 150 mg/L Ca^{2+} and 10 mg/L Fe^{2+} was prepared. The pH value of the solution was adjusted to 9.0 with sodium borax. Then the solution was evenly mixed with a known amount of the

IA/SAS/SHP copolymer. The obtained mixed solution was stirred for 15 min and heated at 50℃ for 5 h before being cooled to room temperature. The transmittance of the supernatant was measured with a 724-spectrophotometer (710 nm, 1 cm cuvette; in relation to distilled water). It was supposed that a smaller light transmittance referred to a better dispersion ability of the copolymer [21,22].

2.5. Corrosion inhibition efficiency of IA/SAS/SHP copolymer

Weight loss of rotating hung steel slices was measured to evaluate the corrosion inhibition efficiency of the IA/SAS/SHP copolymer. The corrosion rate and corrosion inhibition efficiency were determined according to China National Standard GB/T 18175-2000 for "Performance measurement of corrosion inhibitor in water-treatment with a rotating apparatus". The temperature of the system is 50℃, the rotating speed is 75 rpm, and the testing time is 72 h. The carbon steels with surface area of 28 cm^2 were used for corrosion test. The corrosion rate was calculated by Eq. (4) [23].

$$X = \frac{8,760 \times (m_0 - m) \times 10}{S \times t \times D} \tag{4}$$

where m_0 is the mass of carbon steel hung slices before test; m is the mass of carbon steel hung slices after test; S is the surface area of carbon steel hung slice (28 cm^2); t is time of test (72 h); D is density of carbon steel hung slices (7.85 g/cm^3); and 8,760 is a constant which stand for hours of a year (365×24).

The corrosion inhibition efficiency was calculated as:

$$\eta_{\text{corrosion}} = \frac{X_0 - X_1}{X_0} \times 100\% \tag{5}$$

where X_0 is the corrosion rate of the carbon steel in the absence of the IA/SAS/SHP copolymer, mm/a, and X_1 is the corrosion rate of the carbon steel in the presence of the IA/SAS/SHP copolymer, mm/a.

The water used in the test is tap water and the water quality is listed in Table 1.

2.6. Potentiodynamic polarization studies

The polarization measurements were carried out by CH1660B electrochemical workstation with three electrodes, i.e. reference, counter, working electrodes. A saturated calomel electrode (SCE) was used as reference electrode, and all values of potential were referred vs. the SCE. A platinum wire was used as counter electrode [24]. The working electrode was a cylindrical steel specimen that was made from the same rebar as rotating hung steel slices. The anodic and cathodic polarization curves were obtained when stabilization was achieved, after the working electrode was immersed in the test solution for 30 min. Then, the polarization was scanned from a potential 300 mV more negative to the open circuit potential with a constant potential scan rate of 1.0 mV/s.

2.7. Measurement of biodegradability

The biodegradability of the inhibitor is studied by shaking-bottle incubating test. The main methods are as follows: a 500 mL solution with 2 mL inoculum is prepared in a conical flask. The conical flask is placed on a shaking-bottle incubating device at 25℃ and the chemical oxygen demand (COD) is detected at the first, seventh, fourteenth, twenty-first, and twenty-eighth day. The inoculum is prepared by adding 100 g of nutritious soil into 1,000 mL deionized water and filtrating. The ratio of biodegradability of the inhibitor is calculated by Eq. (6):

$$W = \left(1 - \frac{C_t - C_{bt}}{C_0 - C_{b0}}\right) \times 100\% \tag{6}$$

where C_0, C_t, C_{b0}, and C_{bt} represent the initial values of COD in the inoculated solution with the copolymer, the COD value at time t in the inoculated solution with the copolymer, the initial value of COD in the blank solution, the COD value at time t in the blank solution, respectively.

Table 1
Quality of tap water

Total hardness (mg/L)	$[Ca^{2+}]$ (mg/L)	Total alkalinity (mg/L)	$[Cl^-]$ (mg/L)
293.5	186.8	134.6	96.2

3. Results and discussion

3.1. Optimal conditions of IA/SAS/SHP copolymer based on orthogonal experiments

In this work, effects of selected factors were studied through the use of L_9 (3^4) orthogonal experiment and optimal conditions of preparing the IA/SAS/SHP copolymer were obtained (Table 2). The following four variables were analyzed: reaction temperature (factor *A*), reaction time (factor *B*), NaH_2PO_2 concentration (factor *C*) and molar ratio of IA to SAS (factor *D*). The results of the orthogonal experiment are shown in Table 3.

Compared with the range values of different factors (R_j), the factors' levels of significance in this experiment were as follows: reaction temperature > reaction time > molar ratio of IA to SAS > NaH_2PO_2 concentration. The highest inhibition efficiency for each level was clearly distinguished, as the reaction temperature was 90°C, the reaction time was 3.5 h, the NaH_2PO_2 concentration was 11% and the molar ratio of IA to SAS was 4:1, since k_{ji} was the highest at these combinations ($A_1B_1C_3D_2$). The experiment was repeated under the optimal process conditions. Inhibition efficiencies of 95.1% were obtained, which was higher than any former orthogonal experimental result.

3.2. Characterization of IA/SAS/SHP copolymer

3.2.1. FTIR analysis of synthetic products

The FTIR spectra of the reagents and product are shown in Fig. 2. From the spectrum of SAS, the peak at 1,646 cm^{-1} is assigned to the stretching vibration absorption of C=C; the peak at 1,193 cm^{-1} is assigned to the stretching vibration absorption of C–S; the peak at 1,051 cm^{-1} is attributed to the stretching vibration absorption of S=O. From the spectrum of IA, the peak at 1,704 cm^{-1} is assigned to the stretching vibration absorption of C=O; 1,631 cm^{-1} is attributed to the stretching vibration absorption of C=C. while in the spectrum of the product, the peak at 1,686 cm^{-1} is assigned to the stretching vibration absorption of C=O; the peak at 1,403 cm^{-1} is assigned to the vibration absorption of C–P; the peak at 1,270 cm^{-1} is assigned to the stretching vibration absorption of P=O; the peak at 1,137 cm^{-1} is assigned to the stretching vibration absorption of sulfonic acid group. The peak at 995 cm^{-1} is attributed to the stretching vibration absorption of P–O; Stretching vibration absorption peak of C–S is observed at 796 and 620 cm^{-1}. The absence of –C=C– absorption at 1,631 and 1,646 cm^{-1} indicates that the copolymerization of monomers is completed [18], and the product has carboxylic acid group, sulfonic acid group, and phosphino-group.

3.2.2. Molecular weight of IA/SAS/SHP copolymer

The results of viscosity measurements are listed in Table 4. It can be seen from Table 4 that the results of three parallel measurements are highly coincident, which indicates that data obtained from this method are more reliable. The relative molecular weight was 2,381 calculated according to the intrinsic viscosity 0.887.

3.2.3. NMR spectrum of synthetic product

In order to confirm the structure of the synthetic product, ^{31}P NMR and ^{13}C NMR were carried out. Fig. 3(a) is the spectrum of the IA/SAS/SHP copolymer ^{31}P NMR. From the spectrum, the NMR signals—3.405 and 4.219 ppm—were obtained. 3.405 ppm NMR signal was assigned to 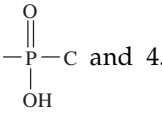 and 4.219 ppm NMR signal was the signal assigned to 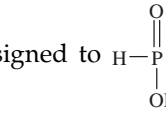 Fig. 3(b) is the spectrum of the IA/SAS/SHP copolymer ^{13}C NMR. The signals obtained in Fig. 4 were 42.881–42.911, 57.421, and 168.068 ppm. 42.881–42.911 ppm

Table 2
Factors and levels of orthogonal experiments

	Factors			
Levels	Reaction temperature (°C) *A*	Reaction time (h) *B*	NaH_2PO_2 concentration (%) *C*	Molar IA:SAS (mol:mol) *D*
1	90	3.5	5	3:1
2	95	4	8	4:1
3	100	4.5	11	5:1

Table 3
Design and results of orthogonal experiments

No.	Factors				Scale inhibition rate (%)
	A	*B*	*C*	*D*	
1	1	1	1	1	92.29
2	1	2	2	2	88.76
3	1	3	3	3	90.53
4	2	1	2	3	91.12
5	2	2	3	1	80.76
6	2	3	1	2	89.94
7	3	1	3	2	87.59
8	3	2	1	3	70.42
9	3	3	2	1	67.25
K_1	271.58	271	252.65	240.30	
K_2	261.82	239.94	247.13	266.29	
K_3	225.26	247.72	258.88	252.07	
k_1	90.53	90.33	84.22	80.10	
k_2	87.27	79.98	82.38	88.76	
k_3	75.09	82.57	86.29	84.02	
R	15.44	10.35	3.91	8.66	

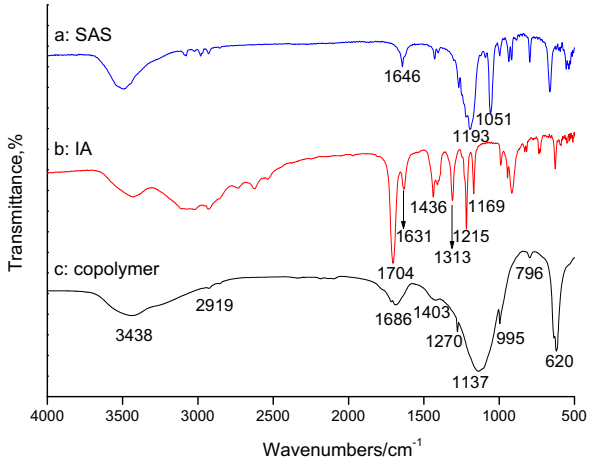

Fig. 2. IR spectra of IA, SAS, and IA/SAS/SHP copolymer.

Table 4
Viscosity of IA/SHP/SAS solution

No.	t_0/s	t/s	η_r	η_{sp}	$[\eta]$
1	131.07	283.50	2.163	1.163	0.885
2	131.12	284.01	2.166	1.166	0.887
3	131.19	284.42	2.168	1.168	0.888
Average	131.13	283.98	2.166	1.166	0.887

Note: t_0: time of standard solution flowing through viscometer; t: time of IA/SHP/SAS solution flowing through viscometer; η_r: relative viscosity; η_{sp}: specific viscosity; $[\eta]$: intrinsic viscosity.

NMR signals were assigned to CH_2. 57.421 ppm NMR signal was the signal of CH. 168.068 ppm NMR signal was the signal of $-\overset{\overset{O}{\|}}{C}-$. There were not the signals of C=C in 120–140 ppm, which is consistent with the result of FTIR analysis. Therefore, the IA/SAS/SHP copolymer was synthesized successfully.

3.2.4. Elemental analysis of synthetic products

The purified IA/SAS/SHP copolymer was analyzed by the elementary instrument and ammonium molybdate spectrophotometric method (measuring the content of phosphorus). Table 5 shows the obtained results. As shown in Table 4, the experimental results of elementary analysis of the IA/SAS/SHP copolymer are found to be in agreement with the calculated ones.

3.3. Inhibition performance of IA/SAS/SHP copolymer against $CaCO_3$

Fig. 4 shows the performance of scale inhibition on $CaCO_3$ in different dosages. The inhibition efficiency in relation to $CaCO_3$ scale increased with an increase in concentration of IA/SAS/SHP copolymer. When the concentration IA/SAS/SHP copolymer was 20 mg/L, the scale inhibition efficiency was 93.4%. The maximum inhibition efficiency, 95.1%, was reached at the copolymer concentration of 24 mg/L.

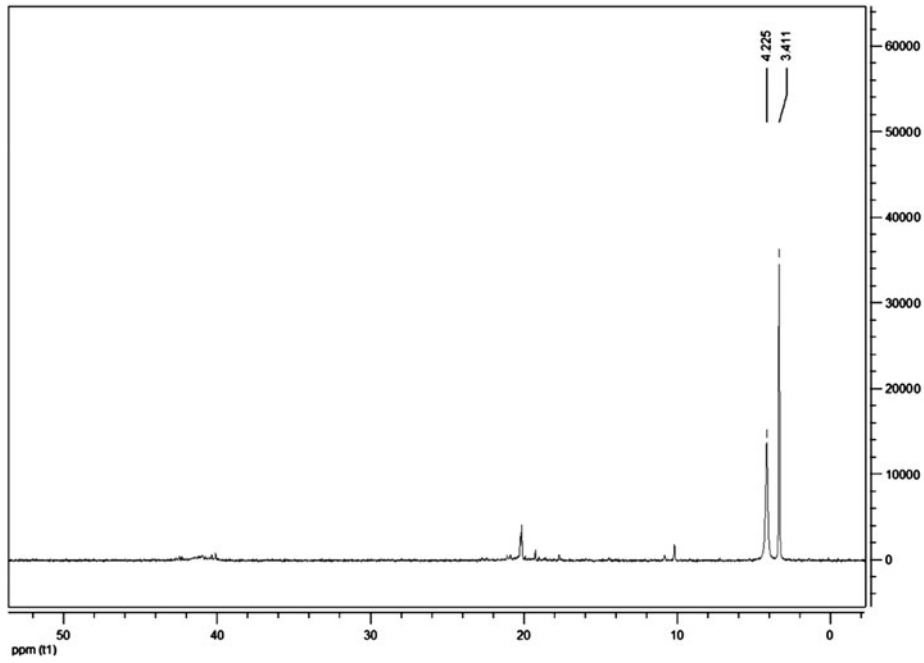

(a) ^{31}P NMR spectrum

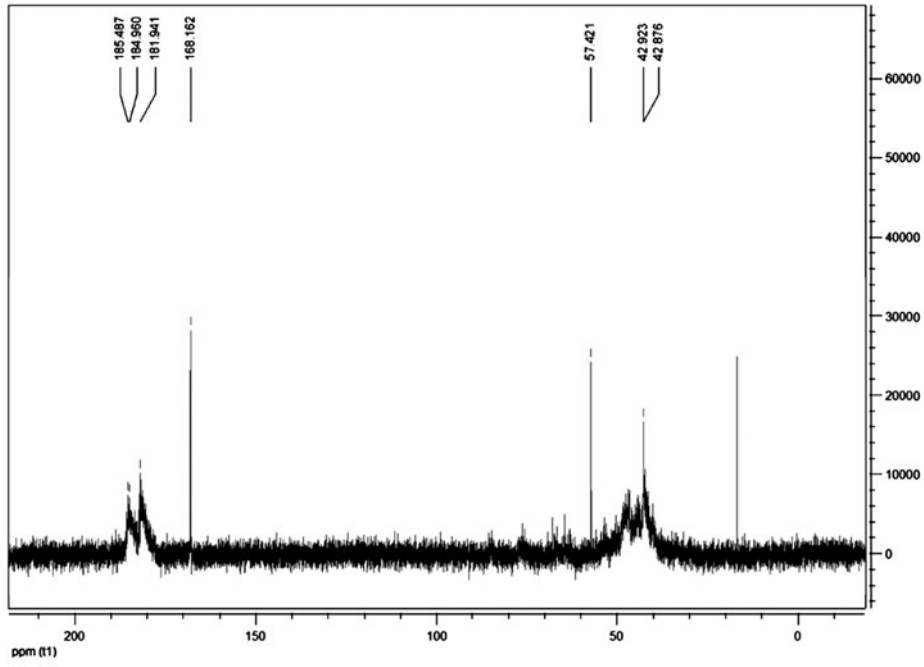

(b) ^{13}C NMR spectrum

Fig. 3. NMR spectra of IA/SAS/SHP copolymer.

And when beyond 24 mg/L, the inhibition efficiency nearly unchanged with the concentration. What should be emphasized is that the solution became transparent and showed no sign of deposition at a copolymer concentration of 20 mg/L. The reason may lie in the copolymer could chelate Ca^{2+} to form

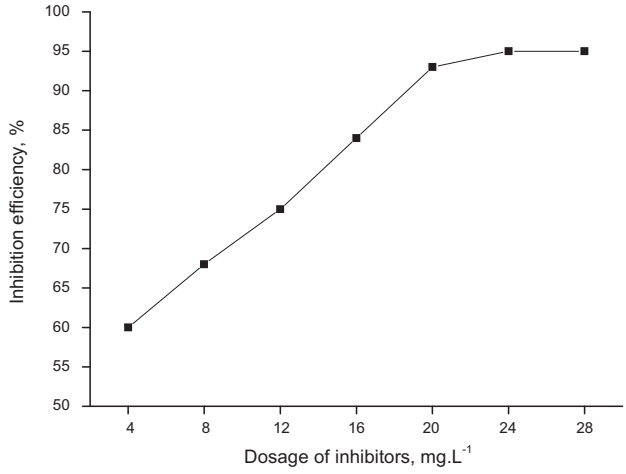

Fig. 4. Inhibition efficiency of IA/SAS/SHP against $CaCO_3$ scale.

Table 5
Data of elemental analysis

		Elemental content (wt.%)			
Chemical		C	H	S	P
IA/SAS/SHP	Theoretical	37.10	4.15	3.93	3.5
	Analytical	36.27	3.98	4.01	3.1

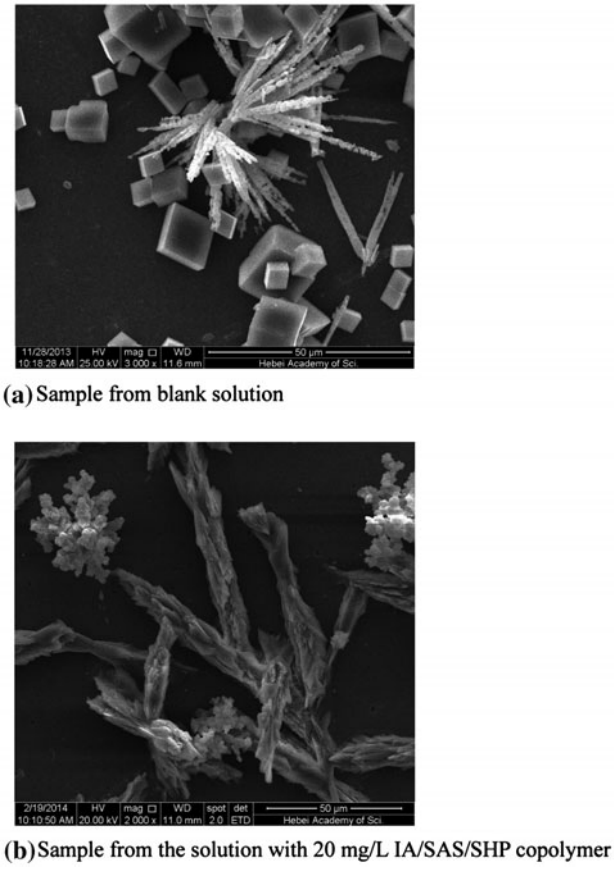

Fig. 5. SEM photograph of $CaCO_3$ samples in the static experiments.

unstabilized and dissoluble chelates to prevent $CaCO_3$ scale from deposition efficiently.

3.4. Morphology of $CaCO_3$ scales formed in the absence and presence of IA/SAS/SHP copolymer

The SEM morphologies of $CaCO_3$ deposits formed in the absence and presence of the IA/SAS/SHP copolymer (20 mg/L) are shown in Fig. 5. $CaCO_3$ deposit formed in the absence of the IA/SAS/SHP copolymer is dense and has a regular shape featuring well-defined cubes and glossy surface (Fig. 5(a)) whereas flower-shaped and cascade-like agglomerated $CaCO_3$ deposits were obtained when the IA/SAS/SHP copolymer was introduced into the solution of $Ca(HCO_3)_2$ (Fig. 5(b)). The difference in the morphology of the $CaCO_3$ deposit is mainly attributed to the presence of the inhibitor which is adsorbed on the crystal surface, reducing their growth rate, destroying crystal habits, and resulting in the crystal distortion. Consequently, the scale was not easy to be attached to the pipe surface [25].

3.5. XRD characterization of $CaCO_3$ crystals formed in the absence and presence of IA/SAS/SHP copolymer

Fig. 6 shows that the diffraction peak strength of the calcite crystal 2θ formed within the blank sample without the IA/SAS/SHP copolymer at 29.301° (the characteristic crystal face 104 of the calcite) and 48.420° (the characteristic crystal face 116 of the calcite) was the strongest, which illustrated that the faces (104) and (116) were the major growth surfaces. The crystal 2θ formed after adding the IA/SAS/SHP copolymer also had the diffraction peaks at 29.301° and 48.420°, but the peak strength was greatly reduced, which indicates that the growth of the crystal faces 104 and 116 is mainly inhibited by the IA/SAS/SHP copolymer and the calcite crystal habits is destroyed. The unstable and dispersed crystal is easy to dissolve and flow with water, but difficult to attach to the surface of the heat exchanger. As a result, the impact on heat transfer can be prevented and the scale inhibition effect can be acquired.

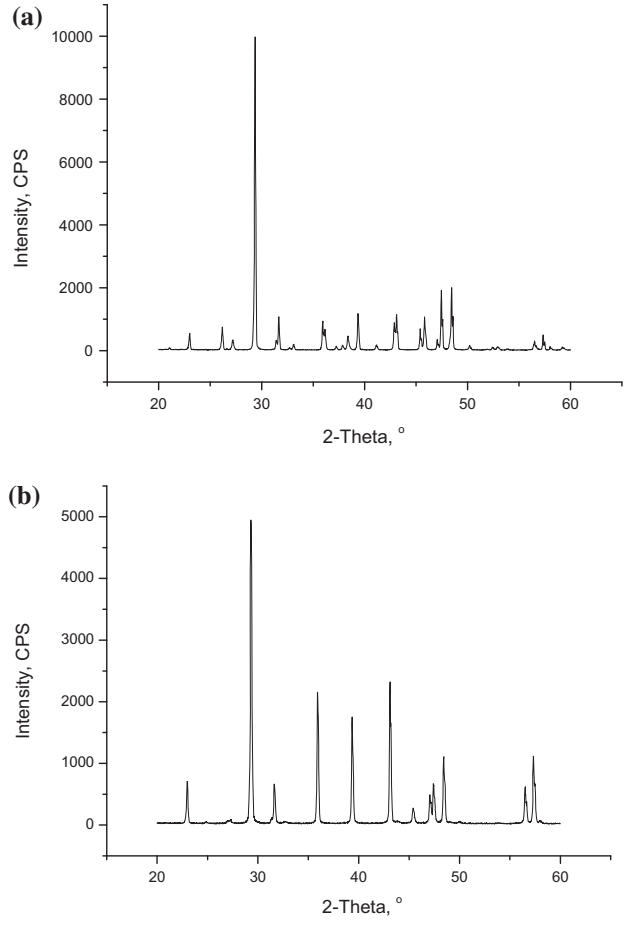

Fig. 6. XRD images of the $CaCO_3$ crystals formed in the absence of inhibitor (a) and in the presence of inhibitor 20 mg/L (b).

3.6. Results of dispersion experiments to ferric oxide

The results of dispersing ferric oxide experiments are shown in Fig. 7. When dosage was below 20 mg/L, the IA/SAS/SHP copolymer had little dispersing performance. However, when the dosage was above 20 mg/L, the dispersion performance improved significantly. When the concentration of IA/SAS/SHP copolymer was 30 mg/L, the transmittance was only 65.7%. It can be seen that the IA/SAS/SHP copolymer has good dispersion capacity for ferric oxide. This is because the IA/SAS/SHP copolymer contains sulpfonic acid group with a high density of electron cloud and is able to coordinate with metal ions to generate stable complex to prevent ferric oxide from precipitation.

3.7. Corrosion inhibition performance

According to the method and conditions of measurement, the corrosion inhibition performances of the

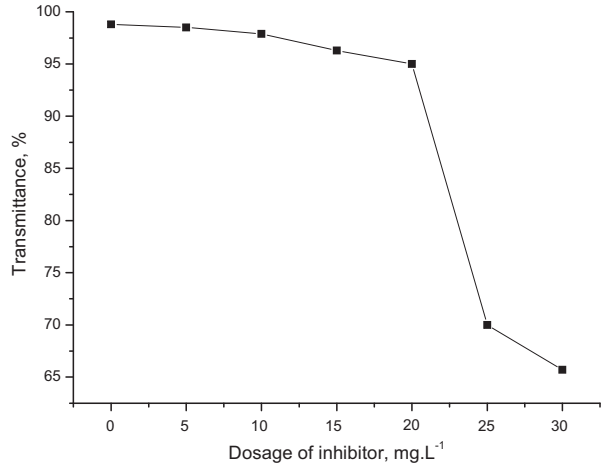

Fig. 7. Dispersion performance of IA/SAS/SHP on Fe_2O_3.

IA/SAS/SHP copolymer in different dosages were evaluated. The results are shown in Table 6.

It was found that the IA/SAS/SHP copolymer had good corrosion inhibition performance. The corrosion inhibition rate significantly increased as the concentration increasing. When the concentration of the IA/SAS/SHP copolymer was 60 mg/L, the corrosion rate was 0.02823 mm/a, and the corrosion inhibition efficiency reached more than 90%. The reason may lie in the copolymer form which chelates with iron ion to protect the surface of test pieces.

3.8. Observation of test pieces

The surface of the test pieces were examined by SEM under the condition of acceleration voltage 20 kV and amplified factor 500. Fig. 8 shows the SEM images of the test pieces. Clear pits were visible due to pitting type of the corrosion specimens in blank solution in SEM images. No obvious pit was visible on the corrosion specimens when 60 mg/L IA/SAS/SHP copolymer was added in solution.

The optical photographs of the pieces taken by SONY DSC-W310 are shown in Fig. 9. No corrosion on A3 carbon steel piece is observed, the surface was very smooth and clear when 60 mg/L scale and corrosion inhibitor was added in solution, as shown in photos. This was because the adsorption of the IA/SAS/SHP copolymer on metal surface was comprehensive. The IA/SAS/SHP copolymer can form chelates with iron ion to protect the surface of test pieces. To sum up, the IA/SAS/SHP copolymer could protect the surface of test pieces very well in solution.

Table 6
Corrosion rates of carbon steel with dosage of the IA/SAS/SHP copolymer

Concentration of IA/SAS/SHP (mg/L)	20	40	60	80	Blank
Corrosion rate (mm/a)	0.2586	0.1157	0.02823	0.01882	0.4107
Corrosion inhibition efficiency (%)	37.04	71.83	93.13	95.42	–

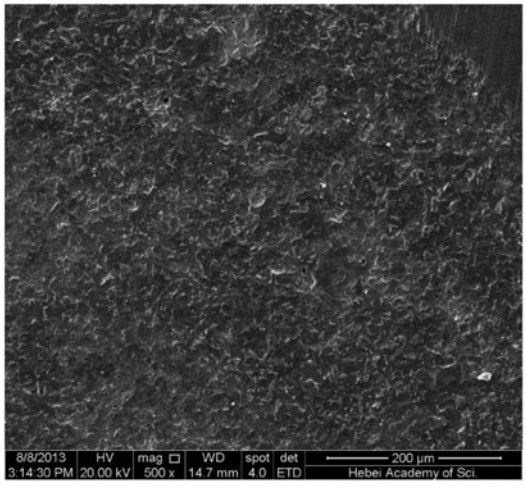

(a) blank solution

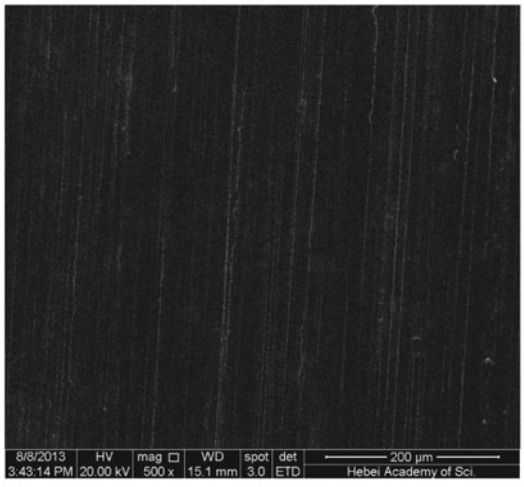

(b) with 60 mg/L IA/SAS/SHP copolymer in solution

Fig. 8. SEM images of test pieces.

(a) blank solution

(b) 60 mg/L IA/SAS/SHP copolymer in solution

Fig. 9. Photographs of test pieces.

The surface elements of the same tested specimens were analyzed by EDS. The results are shown in Fig. 10 and Table 7. When the solution contained IA/SAS/SHP copolymer, the oxygen content in the surface of test piece decreased from 34.02 to 8.47%. The oxygen elements in EDS are mainly from Fe_2O_3 produced in corrosion, so the oxygen element decrease indicates that the surface corrosion reduces. These results are consistent with the photographs in Fig. 9.

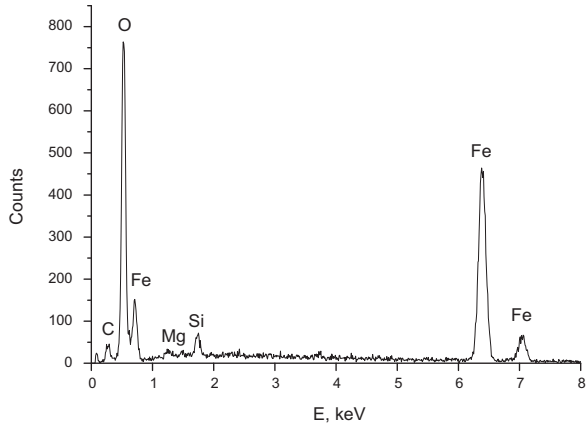

(a) blank solution

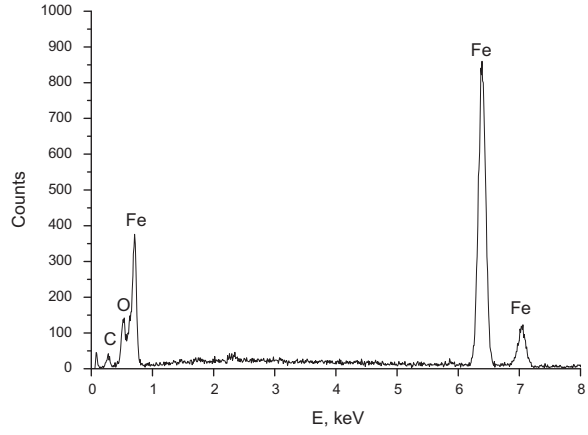

(b) 60 mg/LIA/SAS/SHP copolymer in solution

Fig. 10. EDS diagrams of test pieces.

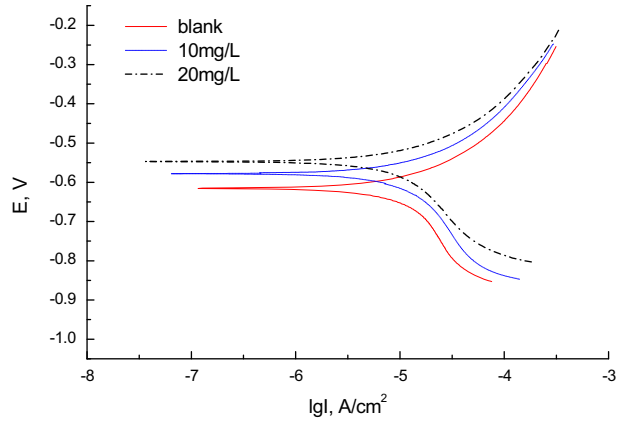

Fig. 11. Tafel polarization curves of A3 steel in the absence and presence of different concentration of the IA/SAS/SHP copolymer in tap water.

The electrochemical parameters derived from Tafel polarization curves are summarized in Table 8. It is indicated that the inhibitors controlled both the anodic and cathodic reactions, but predominantly act as anodic inhibitor [24]. Also, by increasing the concentration of the IA/SAS/SHP copolymer, corrosion current density decreases. It is well known that the corrosion current density (I_{corr}) is related to the corrosion rate, thus it can be concluded that the presence of the IA/SAS/SHP copolymer decreases the corrosion rate and by increasing the concentration of the IA/SAS/SHP copolymer, the corrosion rate decreases. The inhibitor is believed to adsorb at the iron surface and offer a good barrier layer which enhances the iron properties against corrosion.

3.9. Polarization measurement

The analysis of Tafel polarization curves (Fig. 11) was used to determine the electrochemical corrosion kinetics parameters, such as corrosion current density (I_{corr}), and corrosion potential (E_{corr}) [26].

3.10. Results of biodegradation performance

The biodegradability of the IA/SAS/SHP copolymer is shown in Fig. 12. The results show that 52.2% of the copolymer can be biodegraded within 7 d and a value of 69.5% can be reached in 28 d.

Table 7
Content analysis of elements in test pieces

	wt.%	
Elements	Piece in blank solution	Piece in solution with inhibitor
C	6.39	5.89
O	34.02	8.47
Mg	1.37	–
Si	2.50	1.01
Fe	55.72	84.63

Table 8
Electrochemical corrosion parameters of A3 steel in the absence and presence of different concentrations of the IA/SAS/SHP copolymer in tap water

Inhibitor (mg/L)	E_{corr} (mV/SCE)	I_{corr} (μA/cm^2)
Blank	552	36.47
10	546	14.37
20	510	7.59

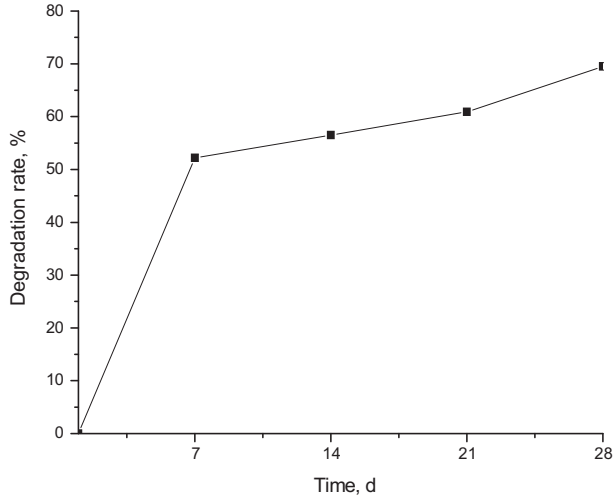

Fig. 12. Biodegradation of the IA/SAS/SHP copolymer.

4. Conclusions

The IA/SAS/SHP copolymer was synthesized and its structure was characterized by means of infrared spectroscopy and elementary analysis. The scale inhibition performance of the IA/SAS/SHP copolymer was evaluated by using static-scale inhibition experiments. The corrosion inhibition and dispersion performance were also examined. It has been found that the IA/SAS/SHP copolymer possesses excellent performance of scale inhibition. This is because the copolymer could destroy the growth habits of the crystal and lead to crystal distortion. Besides, the IA/SAS/SHP copolymer has good corrosion inhibition efficiency. It could form chelates with iron ion to protect the surface of test pieces. In addition, the dispersion and biodegradability of the copolymer is good. The IA/SAS/SHP copolymer is a novel efficient biodegradable multifunctional scale and corrosion inhibitor. It is convenient and economical and it has practical application value.

Acknowledgments

This work was financially supported by the National Natural Science Foundation of China (21376062) and the Natural Science Foundation of Hebei Province (B2011302001) and (B2012302006).

References

[1] B. Zhang, D.P. Zhou, X.G. Lv, Y. Xu, Y.Ch. Cui, Synthesis of polyaspartic acid/3-amino-1H-1,2,4-triazole-5-carboxylic acid hydrate graft copolymer and evaluation of its corrosion inhibition and scale inhibition performance, Desalination 327 (2013) 32–38.
[2] R. Touir, N. Dkhireche, M. Ebn Touhami, M. Lakhrissi, B. Lakhrissi, M. Sfaira, Corrosion and scale processes and their inhibition in simulated cooling water systems by monosaccharides derivatives, Desalination 249 (2009) 922–928.
[3] R. Touir, N. Dkhireche, M. Ebn Touhami, M. Sfaira, O. Senhaji, J.J. Robin, B. Boutevin, M. Cherkaoui, Study of phosphonate addition and hydrodynamic conditions on ordinary steel corrosion inhibition in simulated cooling water, Mater. Chem. Phys. 122(1) (2010) 1–9.
[4] Y.H. Zhang, Zh.F. Liu, W.Zh. Yang, Research on synthesis and performance of itaconic acid homopolymer, Ind. Water Treat. 26(8) (2006) 21–22.
[5] Suharso, Buhani, S. Bahri, T. Endaryanto, Gambier extracts as an inhibitor of calcium carbonate ($CaCO_3$) scale formation, Desalination 265 (2011) 102–106.
[6] F.M. Mahgoub, B.A. Abdel-Nabey, Y.A. El-Samadisy, Adopting a multipurpose inhibitor to control corrosion of ferrous alloys in cooling water systems, Mater. Chem. Phys. 120 (2010) 104–108.
[7] J.B. Sun, G.A. Zhang, W. Liu, M.X. Lu, The formation mechanism of corrosion scale and electrochemical characteristic of low alloy steel in carbon dioxide-saturated solution, Corros. Sci. 57 (2012) 131–138.
[8] A.M. Abdel-Gaber, B.A. Abd-El-Nabey, E. Khamis, D.E. Abd-El-Khalek, A natural extract as scale and corrosion inhibitor for steel surface in brine solution, Desalination 278 (2011) 337–342.
[9] Y.Q. Yu, A.X. Dong, Zh.Zh. Li, Synthesis and application of itaconic acid terpolymer scale inhibitor, Ind. Water Treat. 25(10) (2005) 44–46.
[10] C.M.M. Bougeard, E.H. Goslan, B. Jefferson, S.A. Parsons, Comparison of the disinfection by-product formation potential of treated waters exposed to chlorine and monochloramine, Water Res. 44(3) (2010) 729–740.
[11] Ch. Wang, Sh.P. Li, Calcium carbonate inhibition by a phosphonate-terminated poly(maleic-co-sulfonate) polymeric inhibitor, Desalination 249 (2009) 1–4.
[12] I. Drela, P. Falewicz, S. Kuczkowska, New rapid test for evaluation of scale inhibitors, Water Res. 32(10) (1998) 3188–3191.
[13] D.J. Choi, S.J. You, J.G. Kim, Development of an environmentally safe corrosion, scale, and microorganism inhibitor for open recirculating cooling systems, Mater. Sci. Eng., A 335(1–2) (2002) 228–235.
[14] F.S. de Souza, A. Spinelli, Caffeic acid as a green corrosion inhibitor for mild steel, Corros. Sci. 51(3) (2009) 642–649.

[15] X.L. Wu, Zh.F. Liu, H.H. Li, Research on the synergistic scale inhibition effect of itaconic acid homopolymer with high voltage electrostatic field, Ind. Water Treat. 30(5) (2010) 33–35.
[16] D. Hasson, D. Bramson, B. Limoni-Relis, R. Semiat, Influence of the flow system on the inhibitory action of $CaCO_3$ scale prevention additives, Desalination 108 (1997) 67–79.
[17] E.L. Wang, Research on the synthesis of the copolymer phosphor-containing AA/AMPS and its scale inhibition performance, Ind. Water Treat. 23(3) (2003) 52–53.
[18] X.X. Gu, F.X. Qiu, X. Zhou, J. Qi, Y. Zhou, D.Y. Yang, Q. Guo, X.R. Guo, Synthesis and application of terpolymer scale inhibitor in the presence of β-cyclodextrins, J. Pet. Sci. Eng. 109 (2013) 177–186.
[19] R. Pairat, C. Sumeath, F.H. Browning, H.S. Fogler, Precipitation and dissolution of calcium−ATMP precipitates for the inhibition of scale formation in porous media, Langmuir 13 (1997) 1791–1798.
[20] Y. Xu, L.L. Zhao, L.N. Wang, S.Y. Xu, Y.Ch. Cui, Synthesis of polyaspartic acid–melamine grafted copolymer and evaluation of its scale inhibition performance and dispersion capacity for ferric oxide, Desalination 286 (2012) 285–289.
[21] B.R. Smith, Scale prevention by addition of polyelectrolytes, Desalination 3 (1967) 263–268.
[22] P. Shakkthivel, T. Vasudevan, Acrylic acid-diphenylamine sulphonic acid copolymer threshold inhibitor for sulphate and carbonate scales in cooling water systems, Desalination 197 (2006) 179–189.
[23] A. Stathoulopoulou, K.D. Demadis, Enhancement of silicate solubility by use of "green" additives: Linking green chemistry and chemical water treatment, Desalination 224 (2008) 223–230.
[24] M.A. Abu-Dalo, N.A.F. Al-Rawashdeh, A. Ababneh, Evaluating the performance of sulfonated Kraft lignin agent as corrosion inhibitor for iron-based materials in water distribution systems, Desalination 313 (2013) 105–114.
[25] R. Wang, Q. Zhang, J. Ding, Z.Q. Shen, Survey of researches on scale inhibition mechanism of scale inhibitor, Chem. Ind. Eng. 18 (2001) 79–92.
[26] M.A. Abu-Dalo, A.A. Othman, N.A.F. Al-Rawashdeh, Exudate gum from acacia trees as green corrosion inhibitor for mild steel in acidic media, Int. J. Electrochem. Sci. 7(10) (2012) 9303–9324.